

# PERFORMANCE OF PRESTRESSED CONCRETE BEAM INCORPORATING AN AXIAL YIELD DAMPER USING UNBONDED REBAR

YUKI SHIRAI and KAZUSHI SHIMAZAKI

*Dept of Architecture, Kanagawa University, Yokohama, Japan*

Unbonded prestressed concrete (UBPC) has shown considerable promise for structural elements in continuous-use applications. However, little research has evaluated the performance of UBPC structural elements or their low energy absorption ability, and such elements are therefore not commonly used as main structural members. In this study, a small axially yielding hysteresis damper was developed, which can be replaced in the event of earthquake damage to a UBPC beam in high continuous use. The damper was designed to use the axial yielding of deformed rebars so that it has the same performance under compressive and tensile forces. It was mounted in a knee brace shape and had a mass of about 10 kg. The damper exhibited positive and negative hysteresis characteristics even after the deformed rebars had yielded axially and it had sufficient energy absorption capacity. In a structural experiment, installing the damper, the shear force that can be borne by the beam and the equivalent damping constant increased, which means that the damper is useful.

*Keywords:* Continuous usability, Sustainable, Earthquake resistance, Vibration resistance.

## 1 INTRODUCTION

Prestressed concrete structures using ultra high strength steel that is not bonded to the concrete (hereinafter, unbonded prestressed concrete, UBPC) suffer little damage during earthquakes and little concentrated damage near joints between structural members. However, the energy absorption capacity of UBPC structural members is low, and therefore deformation may increase during an earthquake (Okamoto and Katoh 1983). Previously, Shirai and Shimazaki (2020) investigated UBPC frames equipped with viscoelastic dampers.

In this study, a damper was developed that can be attached to the end of a UBPC beam, where deformation and damage are concentrated, and the performance of the beam with the damper attached was evaluated in a structural experiment.

## 2 SMALL DAMPER USING UNBONDED REBAR

A compact, lightweight damper was developed that can be easily attached and detached by debonding the deformed rebar used in a previous study by Shimazaki *et al.* (2011).

## 2.1 Overview of the Experiment

Table 1 lists the experimental parameters, and Figure 1 shows the specimen shape and gives its dimensions. There were seven specimens in total. The parameters are the embedded depth and the type of mortar used as the restraining material. For each test piece, the inner rebar was friction welded at each of its ends to outer rebar. The test specimens were designed based on a comparison of the yield strength of the outer rebar and the tensile strength of the inner rebar.

Table 1. Specimen experimental parameters of the damper.

Specimen	Embedded Depth of Outer Rebar	Inner Rebar (Bamboo-shaped)	Outer Rebar (Screw-shaped)	Mortar	Weight [kg]
1	6d	D16 SD345	D22 SD390	A	12
2	4d			A	10
3				B	12
4				A	9
5	2d			B	11
6	4.5d	D19 SD345	D25 SD390	A	7
7				B	8

d: diameter of the outer rebar

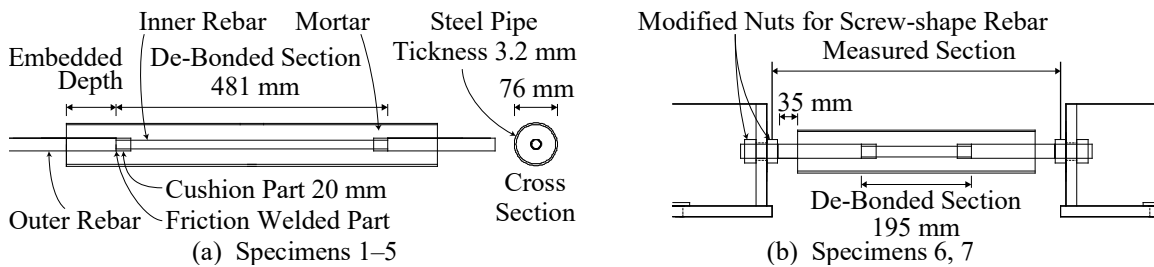


Figure 1. Specimens shape and dimensions.

In the process of debonding the core material, which consists of the outer and inner rebar, the outer rebar was filled with clay and the inner rebar and the outer rebar were covered with a hard vinyl sheet, which was then adhered to the core material with a heat-shrinkable tube. The core material was surrounded by a steel pipe with an outer diameter of 76.3 mm and a thickness of 3.2 mm, and the gap between the core material and the outer steel pipe was filled with mortar. The clearance provided by the thickness of the heat-shrinkable tube was 0.7 mm. Table 2 lists the properties of the materials used.

Table 2. Material characteristics of the damper.

Mortar	Compressive Strength [N/mm <sup>2</sup> ]	Rebar	Yield Strength [N/mm <sup>2</sup> ]	Tensile Strength [N/mm <sup>2</sup> ]
		A	100.6	D16 SD345
B	111.3	D19 SD345	382	552
		D22 SD390	475	612
		D25 SD390	453	588

Figure 2 shows the loading setup. One end of the specimen was fixed to a horizontally movable jig, connected to an actuator, and pushed and pulled in the axial direction of the specimen. The load cycle was positive for tension and negative for compression, and each of 1/3

$P_y$ ,  $2/3 P_y$ , and  $P_y$  of the yield loads of the inner rebars were applied negatively and positively once. After that, for specimens 1–5, positive and negative increasing forces were repeated twice, with each horizontal displacement being  $\pm 5$  mm. Specimens six and seven were prepared for a structural experiment. The load was applied until the rebar buckled, strength reduction occurred due to buckling of the neck at the friction welded part, or tensile fracture occurred.

As shown in Figure 1, the total displacement in the axial direction of the test specimen and the strain of the inner rebar were measured.

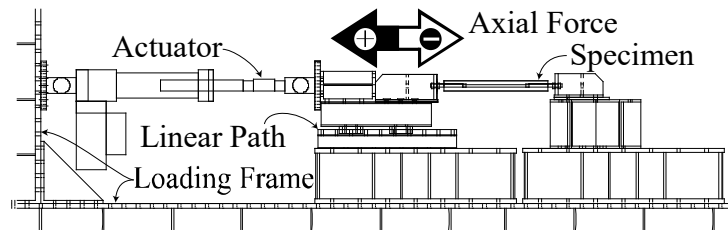


Figure 2. Loading setup of the damper.

## 2.2 Experimental Results

The strain distribution of the inner rebar demonstrated that the inner rebar was uniformly tensioned and compressed within the elastic range by the debonding.

Table 3 lists the experimental results for each specimen, and Figure 3 shows the examples of failure modes. All of the test pieces exhibited tensile fracture at or near the friction weld. In all the test pieces, one of the cushioning materials was crushed, which means that the deformation was concentrated on one side.

Table 3. Experimental results.

Specimen	Failure mode	Buckling Mode	$E_t$	$\omega$	$\alpha$	$P_t$	$P_c$
1	Tensile Fracture	0	2.9	25.5	0.96	94.5	90.4
2		13	44.3	389	1.5	119	179
3		13	41.9	368	1.53	119	182
4	Buckling at Friction Weld	11	25.9	227	1.3	114	148
5		9	27.1	238	1.45	116	169
6	Buckling of Outer Rebar	5	22.5	501	1.17	162	190
7	Tensile Fracture	5	24	533	1.13	165	187

$E_t$ : cumulative plastic strain energy;  $\omega$ : cumulative plastic strain energy ratio;  $\alpha$ : compression-to-tension strength ratio;  $P_t$ : tension strength;  $P_c$ : compressive strength.

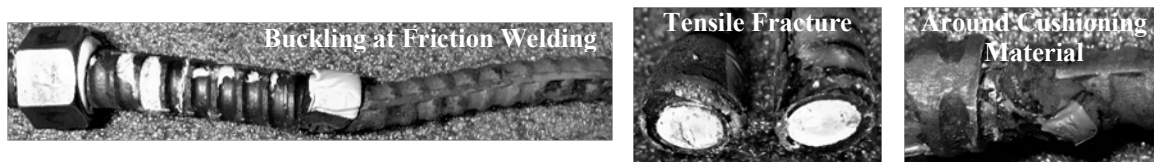


Figure 3. Failure modes.

Figure 4 shows the relationship between axial load and axial deformation of a representative specimen. In specimen two, the yield deformation during compression was concentrated between the deformed rebars. The compressive stress increased because of volume expansion due to the Poisson effect and frictional force due to contact with the restraining material as a result of the inner rebar having a higher buckling mode. When plotted, the relationship for specimens six and seven is generally a stable loop.

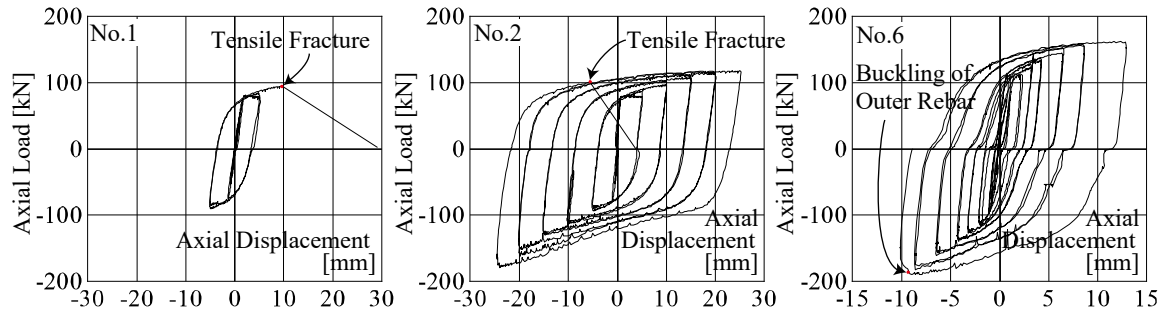


Figure 4. Relationship between axial load and displacement.

Table 3 shows values of  $E_t$ ,  $\omega (= E_t / P_y \cdot \delta_y$ , where  $P_y$  is the yield load of the inner rebar and  $\delta_y$  is elastic deformation), and the compression-to-tension strength ratio  $\alpha (= P_C / P_T)$ .  $\omega$  is a large value because the specimen with the embedded depth of  $4d$  did not buckle or break in the outer rebar portion.

The compression-to-tension strength ratio  $\alpha$  is smaller in specimens six and seven than in specimens one to five. The difference in the cross-sectional area between the nodes of the inner rebar is larger in specimens six and seven than in specimens one to five. Therefore, the transmission of force to the restraining material due to the cross-sectional area expansion at the time of compression yielding was reduced.

### 3 STRUCTURE EXPERIMENT

The purpose of this section is to report the damper's performance when it is attached to unbonded prestressed concrete (UBPC) beams.

#### 3.1 Overview of the Experiment

Table 4 lists the material characteristic of the member specimens, and Figure 5 illustrates the shape of the specimens. Test specimens were assumed to be 40% of the size of an actual member and consisted of a beam part and a precast stub. The shear span is a cantilever beam with a depth ratio of 3.5 for from the beam end to the center of the beam span. This experiment investigated the results with and without the damper. The bar was prestressed concrete and was tensioned and fixed via spherical support and the load cell.

Table 5 lists the material properties. In the experiment, the concrete compressive strength  $\sigma_B$  was about  $60 \text{ N/mm}^2$ . The axial and shear rebars were SD295A.

Figure 5 illustrates the experimental setup. The stub was fixed to the load frame, and the shear force  $Q$  was applied to the test piece by the actuator connected via the load jig. Loading was applied by controlling the deformation, and the member drift angle  $R$  was 0.125, 0.25, 0.5, 0.75, 1.0, 1.5, and 2.0 %rad, applied three times positively and three times negatively, and 3 and 4 %rad, applied once positively and once negatively.

Table 4. Specimen experimental parameters of member specimens.

Specimen	Cross Section Width×Depth [mm×mm]	Shear Span to Depth Ratio L/D [-]	Prestress $\sigma_g$ [N/mm <sup>2</sup> ]	Design Shear Strength		
				Flexural Crack $Q_c$ [kN]	Ultimate Shear Strength $Q_u$ [kN]	Ultimate Flexural Strength $Q_{mu}$ [kN]
1	220×400	3.5	11.9	80	221	149
2			11.6			

Table 5. Material characteristics of member specimens.

Concrete F <sub>c</sub> =48 N/mm <sup>2</sup>	Compressive Strength [N/mm <sup>2</sup> ]	Split Tensile Strength [N/mm <sup>2</sup> ]	Young's Modulus [×10 <sup>3</sup> N/mm <sup>2</sup> ]	Rebar	Yield Strength [N/mm <sup>2</sup> ]	Tensile Strength [N/mm <sup>2</sup> ]
	$\sigma_b$	$\sigma_t$	$E_c$			
1	60.7	15.9	32.9	D16 SD345	394	585
2	60.9	16.7	32.7	D19 SD345	382	552
				D22 SD390	475	612
				D25 SD390	453	588

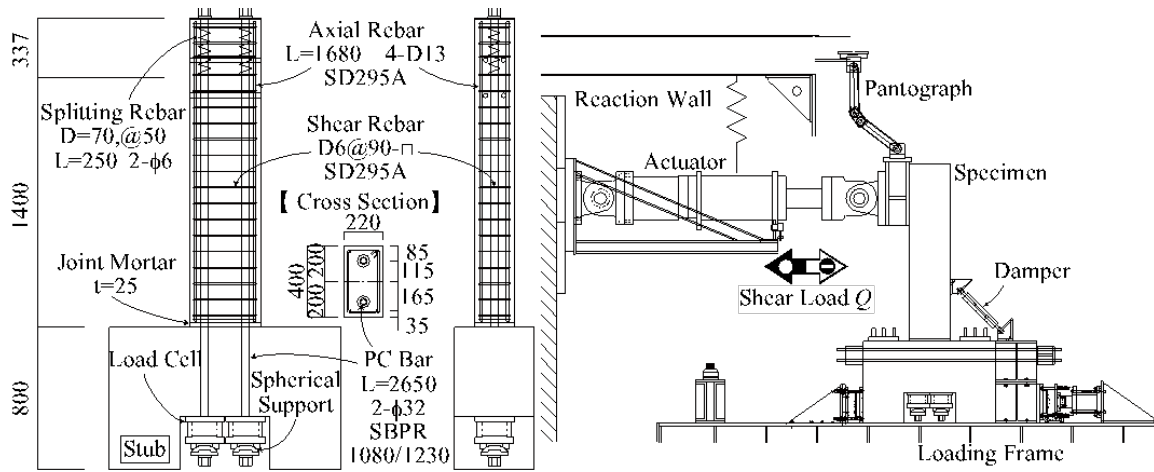


Figure 5. Specimens shape and dimensions, and loading setup of the member.

The out of plane direction is restrained by a pantograph connected to a load jig. Measurements were taken of the shear force  $Q$ , member drift angle  $R$ , strain of axial and shear rebars, and displacement of the damper fixing jig.

The maximum strength of the test piece was designed to be determined by the compressive fracture of concrete, and the shear force  $Q$  at the end of the bending was 149 kN. The horizontal component of the yield strength of the damper shaft in the material test was 77 kN.

### 3.2 Experiment Results

Figure 6 shows the relationship between shear force  $Q$  and member drift angle  $R$ . The maximum shear force of the specimen without a damper was 160 kN at  $R = 6.8$  %rad. The maximum shear force of the test specimen with the damper was 216 kN. After that, the damper tensile-ruptured in the middle of  $R = + 4$  %rad and the value of  $Q$  decreased, and the same response as the specimen without a damper was then plotted.

The curves plotted in the figure demonstrate that the shear force  $Q$  and the stiffness were increased by adding the damper. The maximum shear force up to a member angle of  $R = 2$  %rad

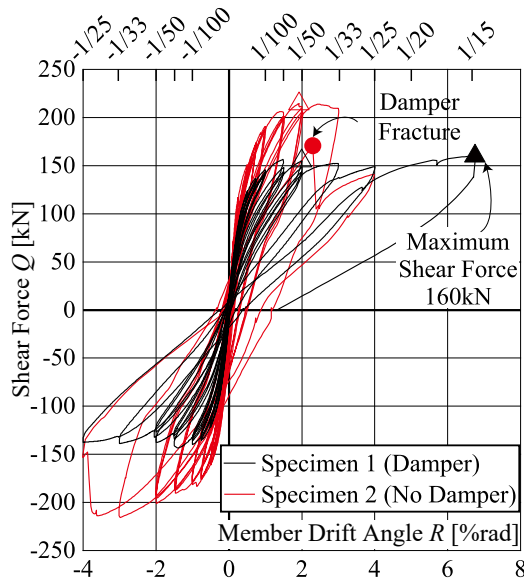


Figure 6. Relationship between axial load and displacement.

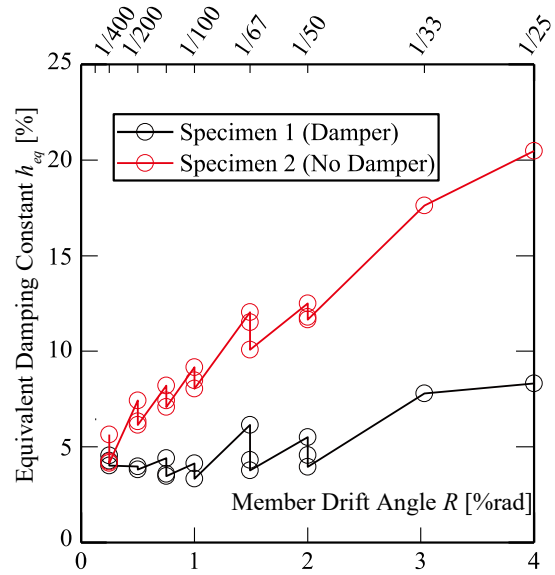


Figure 7. Relationship between member drift angle and equivalent damping constant.

was 155 kN for specimen one and 216 kN for specimen two, which is a difference of 61 kN. The reason for the horizontal component of the yield strength of the damper being 61 kN, which is smaller than 77 kN, can be attributed to the bending moment acting on the damper in addition to the axial force and the fixing jig slipping.

Figure 7 shows the relationship between member drift angle  $R$  and equivalent damping constant  $h_{eq}$  in each cycle from  $R = 1/400$ . The value of  $h_{eq}$  was reduced by repeating it all cycles for both specimens. For the specimen with the damper compared with the one without the damper,  $h_{eq}$  was 1.6 times greater at  $R = 0.5$  %rad and 1.9 times greater at  $R = 1$  %rad.

#### 4 CONCLUSION

In this experiment, a small damper with a cumulative plastic strain energy ratio of about 360 or more was realized by setting the embedded depth to  $4d$ .

The results demonstrate that adding a small axially yielding hysteresis damper, which can be replaced in the event of earthquake damage to a UBPC beam in high continuous use, increases the beam's energy absorption capacity. However, further study is required on the mounting method.

#### References

- Okamoto, S., and Katoh, H., *Earthquake Response Characteristics of Prestressed Concrete Buildings*, Summaries of Technical Paper of Annual Meeting, Architectural Institute of Japan, 2575-2576, Hokuriku, Japan, 1983.
- Shimazaki, K., Ninomiya, S., and Igarashi, I., Experimental Study on Reinforced Concrete Brace Dampers Using De-Bonded Deformed Bars, *AJ Journal of Technology and Design*, 17(35), 157-160, Feb., 2011.
- Shirai, Y., and Shimazaki, K., *Evaluation by Static Loading and Dynamic Loading Experiments —Horizontal Loading Performance of Unbonded PC Frames Assembled by Post-Tensioning with Viscoelastic Damper Part 1—*, *AJ Journal of Technology and Design*, 26(62), 136-140, Feb., 2020.